The Astrophysical Journal, 978:120 (6pp), 2025 January 10 https://doi.org/10.3847/1538-4357/ad9b7c

B2 1308+326: A Changing-look Blazar or Not?

Ashwani Pandey[1,2,3,10], Chen Hu[1], Jian-Min Wang[1,4,5], Bożena Czerny[3], Yong-Jie Chen[1,6], Yu-Yang Songsheng[1], Yi-Lin Wang[1,7], Hao Zhang[1,7], and Jesús Aceituno[8,9]

[1] Key Laboratory for Particle Astrophysics, Institute of High Energy Physics, Chinese Academy of Sciences, 19B Yuquan Road, Beijing 100049, People's Republic of China; ashwanitapan@gmail.com
[2] Department of Physics and Astronomy, University of Utah, Salt Lake City, UT 84112, USA
[3] Center for Theoretical Physics, Polish Academy of Sciences, Al.Lotnikov 32/46, PL-02-668 Warsaw, Poland
[4] School of Astronomy and Space Science, University of Chinese Academy of Sciences, Beijing 100049, People's Republic of China
[5] National Astronomical Observatories of China, The Chinese Academy of Sciences, 20A Datun Road, Beijing 100020, People's Republic of China
[6] Dongguan Neutron Science Center, 1 Zhongziyuan Road, Dongguan 523808, People's Republic of China
[7] School of Physical Science, University of Chinese Academy of Sciences, 19A Yuquan Road, Beijing 100049, People's Republic of China
[8] Centro Astronomico Hispano Alemán, Sierra de los filabres sn, E-04550 Gergal, Almería, Spain
[9] Instituto de Astrofísica de Andalucía (CSIC), Glorieta de la astronomía sn, E-18008 Granada, Spain
Received 2024 September 30; revised 2024 November 27; accepted 2024 December 04; published 2024 December 31

Abstract

In our previous study, we identified a shift in the synchrotron peak frequency of the blazar B2 1308+326 from $10^{12.9}$ to $10^{14.8}$ Hz during a flare, suggesting it could be a changing-look blazar (CLB). In this work, we investigate the changing-look behaviour of B2 1308+326 by analysing a newly acquired optical spectrum and comparing it with an archival spectrum. We find that between the two epochs, the continuum flux increased by a factor of ~4.4, while the Mg II emission line flux decreased by a factor of 1.4 ± 0.2. Additionally, the equivalent width of the Mg II line reduced from ~20 to ~3 Å, indicating an apparent shift from a flat-spectrum radio quasar (FSRQ) class to a BL Lacertae (BL Lac) class. Despite this apparent change, the ratio of accretion disk luminosity to Eddington luminosity remains $>10^{-2}$ during both epochs, indicating efficient accretion persists in B2 1308+326. The measured black hole mass remains consistent with an average $\log M_{\rm BH} = 8.44\, M_{\odot}$. Our findings suggest that B2 1308+326 is not a genuine CLB but rather an intrinsic FSRQ that emerges as a BL Lac during high-flux states due to enhanced nonthermal emission.

Unified Astronomy Thesaurus concepts: Flat-spectrum radio quasars (2163); Blazars (164); Active galactic nuclei (16); Radio loud quasars (1349); Relativistic jets (1390)

1. Introduction

Broad emission lines (BELs) and the underlying thermal continuum from the accretion disk (AD) are the two key components of the UV/optical spectra of active galactic nuclei (AGN). These emission lines are formed due to the photoionization of broad-line region (BLR) clouds by the incident continuum and are Doppler broadened. Based on the existence or lack of BELs in the spectra, AGN are generally divided into Type 1 and Type 2 AGN (e.g., R. Antonucci 1993). However, over the last 10 years, an increasing number of sources have been discovered to exhibit a transition between Type 1 and Type 2 AGN and are referred to as changing-look AGN (CLAGN). The change in their spectral states is mostly due to the change in the underlying incident continuum from the AD, but it could also be due to the change in the line-of-sight column density (see C. Ricci & B. Trakhtenbrot 2023 for an excellent review).

Jetted AGN[11] have an additional, highly variable, nonthermal continuum component due to the synchrotron emission by relativistic electrons within the jet that can affect their UV/optical spectra. Blazars are jetted AGN with jets oriented closer to the observer (C. M. Urry & P. Padovani 1995). They are usually categorized into flat-spectrum radio quasars (FSRQs) and BL Lacertae objects (BL Lacs) based on their UV/optical spectra; FSRQs have BELs (EW $>$ 5 Å) in their spectra, while the spectra of BL Lacs are mostly featureless (J. T. Stocke et al. 1991). A physical distinction between these two categories of blazars is proposed by G. Ghisellini et al. (2011) based on the ratio of disk luminosity ($L_{\rm AD}$) to the Eddington luminosity ($L_{\rm Edd}$). They suggested that BL Lacs have radiatively ineffective accretion ($L_{\rm AD}/L_{\rm Edd} < 10^{-2}$) and hence no emission lines, while in FSRQs, accretion is radiatively efficient, producing BELs in their spectra. The peak, ν_p, of the low energy (synchrotron) component of the spectral energy distributions (SEDs) of blazar is another factor used to classify them. Based on ν_p, blazars are categorized as low-synchrotron peaked (LSP; $\nu_p \leqslant 10^{14}$ Hz), intermediate-synchrotron peaked (ISP; $10^{14} < \nu_p < 10^{15}$ Hz), and high-synchrotron peaked ($\nu_p \geqslant 10^{15}$ Hz) blazars (A. A. Abdo et al. 2010).

Similar to CLAGN, a number of blazars that transitioned from one blazar class to another over various observation epochs have been identified using changes in the emission-line widths and also using shifts in the synchrotron peak frequency (e.g., G. Ghisellini et al. 2011, 2013; J. J. Ruan et al. 2014; H. D. Mishra et al. 2021; A. Pandey et al. 2024; S. Paiano et al. 2024). However, it is still unclear whether these sources are genuine changing-look blazars (CLBs) or whether the transition is apparent because of increased jet continuum emission. During periods of high activity, the enhanced nonthermal jet continuum could swamp out the emission lines in the FSRQ

[10] PIFI visiting scientist.
[11] AGN having strong relativistic jets (P. Padovani 2017).

spectrum, giving the impression that the source is a BL Lac (e.g J. J. Ruan et al. 2014). Similarly, a change in the Doppler factor, most likely due to a change in the viewing angle, could also shift the synchrotron peak (e.g., A. Pandey et al. 2024).

B2 1308+326 (OP 313) is a high-redshift blazar located at $z = 0.9980 \pm 0.0005$ (P. C. Hewett & V. Wild 2010). In our previous work, A. Pandey et al. (2024; hereafter Paper I), we examined the multiwavelength emission of B2 1308+326. Using broadband SED modeling, we found that its synchrotron peak, ν_p, shifted from $10^{12.9}$ (in the low state) to $10^{14.8}$ Hz (in the high state), indicating a change from LSP to ISP class. This encourages us to investigate its spectral characteristics to validate the transitional behavior. In this work, we examined any variation in the emission-line characteristics and underlying continuum flux of B2 1308+326 using two optical spectra (in the observed frame) obtained during different epochs.

The outline of this paper is as follows: Section 2 describes the observations and data reduction process. Results are given in Section 3. We discuss our findings in Section 4, and a summary of the work is presented in Section 5.

2. Observations and Data Reduction

We examined two spectra of B2 1308+326—one archival Sloan Digital Sky Survey (SDSS) spectrum[12] and one new observation with the Centro Astronómico Hispano-Alemán (CAHA) telescope. The archival SDSS spectrum was taken on 2006 March 25 (MJD 53819) and corresponds to plate ID 2029 and fiber number 602. The new observation was performed on 2024 June 18 (MJD 60479) at the Calar Alto Observatory. Two spectra of 1200 s each were taken under good weather conditions using the Calar Alto Faint Object Spectrograph mounted on the 2.2 m CAHA telescope. The Grism G-200 and a long slit set to a projected width of 3.″0 were employed. The night was a photometric night with a recorded seeing of 1.″2 when the spectra were acquired. However, we did not take any images during these observations. We obtained two spectrophotometric standards—one (BD+26 2606) at the beginning and one (BD+28d4211) at the end of the same night. The sensitivity curves from these standards show a minor difference of approximately 0.1 mag. Additionally, four other objects observed that night for our reverberation mapping campaign were calibrated using the same spectrophotometric standards as this target. A comparison of their fluxes with those calibrated using a simultaneously observed comparison star (for our reverberation mapping) showed differences of 15%, 10%, 6%, and 2% for the four objects (e.g., C. Hu et al. 2021). Considering these comparisons, it is reasonable to say that our absolute flux calibration for this target has an accuracy of about 10%. The data reduction was performed by the IRAF[13] following the standard procedures. The reduced spectra cover the wavelength range of ~4000–8500 Å with a dispersion of 4.47 Å pixel^{-1}. The instrumental broadening is ~1000 km s^{-1}, estimated by C. Hu et al. (2020) for the same set of Grism and slit width. These spectra are nearly identical, except for a difference in the shape in the extreme blue region around 4000 Å. Additionally, telluric absorption lines appear at longer wavelengths, specifically beyond 6500 Å. The wavelength range between 4500 and 6500 Å shows good-quality data and is used for further analysis. We plotted the two CAHA spectra taken on MJD 60479 in Figure 1. Each CAHA spectrum has a signal-to-noise ratio (S/N) of approximately 60 at the continuum around the Mg II line. By combining the two spectra, we achieved an improved S/N of ~85. Figure 2 illustrates a direct comparison between the observed SDSS and CAHA spectra spanning the wavelength range of 4500–6500 Å, which includes good-quality data and is used for further investigations.

3. Results

To examine the spectral characteristics of B2 1308+326, we first corrected both SDSS and CAHA spectra for Galactic extinction.[14] We then shifted the observed spectra to the rest frame. The rest-frame spectra of B2 1308+326 have Mg II as the most prominent emission line. Finally, we performed the spectral fitting to both spectra to compute their different spectral components using the algorithm described in Appendix A of C. Hu et al. (2012). Our model is similar to that used in C. Hu et al. (2008) and includes the following components: (1) the AGN continuum (a single power law (PL) of the form $F_\lambda \propto \lambda^{\alpha}$); (2) the Fe II pseudocontinuum (modeled from the M. Vestergaard & B. J. Wilkes 2001 template); (3) the Mg II $\lambda\lambda$2796,2803 doublet (multi-Gaussian).

For the SDSS spectrum, each of the Mg II doublets is modeled using a pair of Gaussian functions: one representing the narrow component and the other capturing the broad component of the doublet (e.g., C. Hu et al. 2008; Y. Shen et al. 2011). However, for the CAHA spectrum, a single Gaussian is enough for each doublet due to its relatively low spectral resolution. The doublets are forced to have the same widths and shifts, while the intensity ratio between them is fixed to the value of 2 (J. A. Baldwin et al. 1996). The FWHM of the Mg II line is calculated from the best-fit model of one of the Mg II doublets. We corrected the observed FWHM of the Mg II line for the instrumental broadening using the following equation:

$$FWHM_{\rm corrected} = \sqrt{\rm FWHM^2_{observed} - FWHM^2_{instrumental}}. \quad (1)$$

The values of instrumental broadening for the SDSS and CAHA spectra are ~167 and ~1000 km s^{-1}, respectively. The results of spectral fitting to the SDSS and CAHA spectra are presented in the left and right panels of Figure 3, respectively. The corresponding fitting parameters are listed in Table 1.

We also estimated the Mg II line flux using a simple integration method for the CAHA spectra, shown in the Appendix. The resulting integrated flux is $(7.3 \pm 0.4) \times 10^{-15}$ erg cm^{-2} s^{-1}, which is slightly lower than the value obtained from the multiple Gaussian fitting. This difference could be due to overestimating the continuum level as the Fe II emission was not subtracted, which significantly influences the observed flux around the Mg II line (e.g., M. Vestergaard & B. J. Wilkes 2001; J. A. Baldwin et al. 2004; A. Pandey et al. 2024). Therefore, we proceed with the results of our fitting method.

We can estimate the virial mass of a black hole using the FWHM of the Mg II line and the continuum luminosity as (e.g.,

[12] Taken from https://cas.sdss.org/dr18/VisualTools/quickobj.

[13] IRAF is distributed by the National Optical Astronomy Observatories, which are operated by the Association of Universities for Research in Astronomy, Inc., under a cooperative agreement with the National Science Foundation.

[14] A value of 0.039 for the V-band extinction magnitude from the NASA/IPAC Extragalactic Database (E. F. Schlafly & D. P. Finkbeiner 2011) was used.

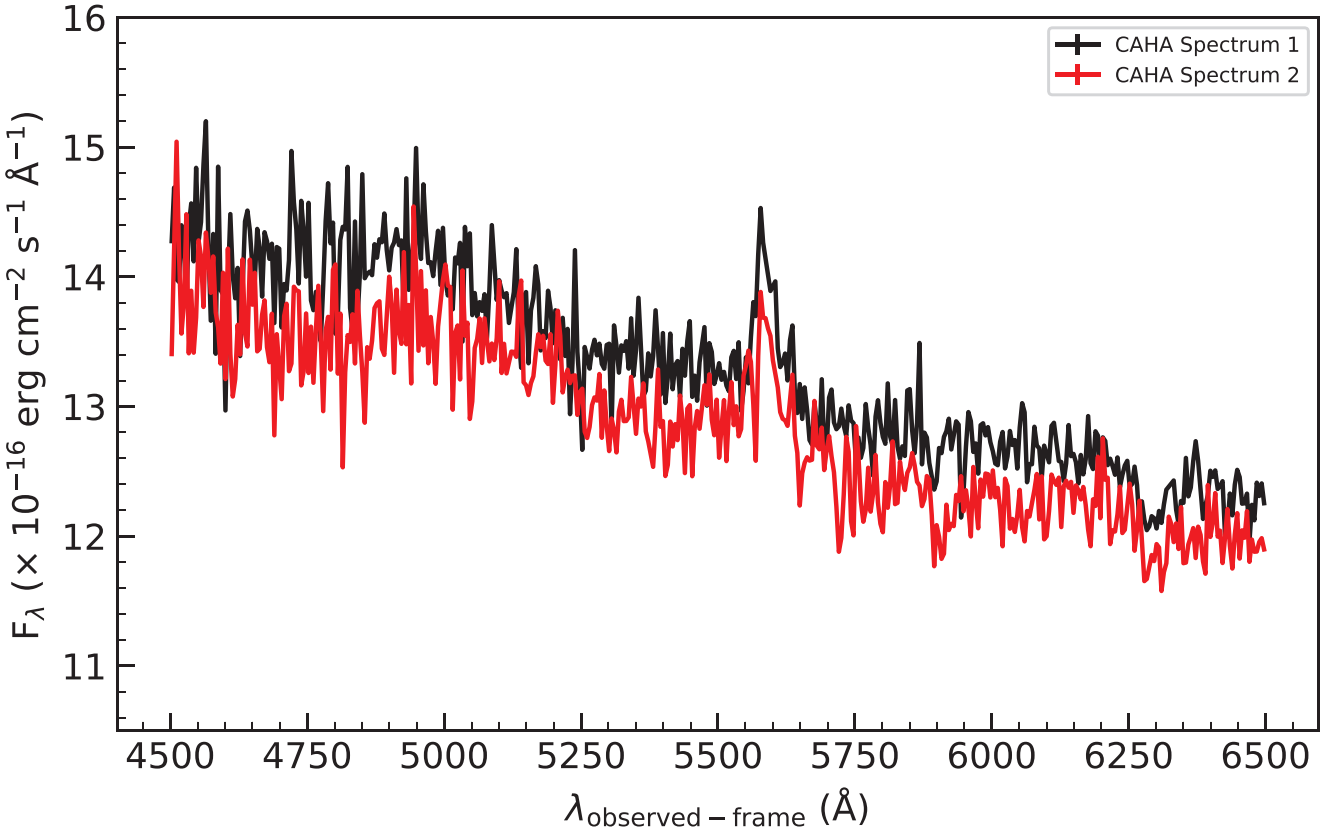

Figure 1. A comparison of two CAHA spectra, each with an exposure time of ~1200 s, taken on MJD 60479. We limited the spectra to the wavelength range of 4500–6500 Å as it contains high-quality data.

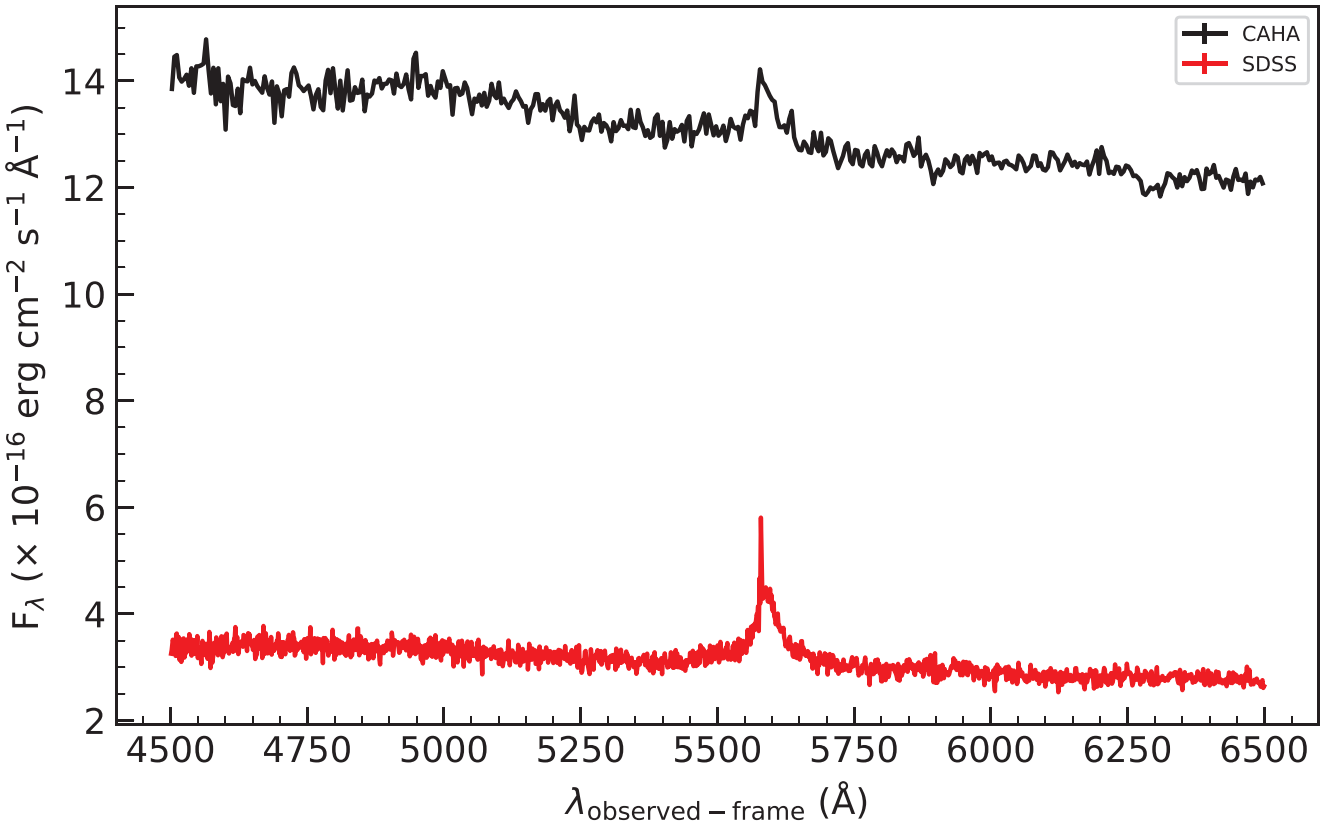

Figure 2. A comparison of observed SDSS and CAHA spectra over the wavelength range 4500–6500 Å.

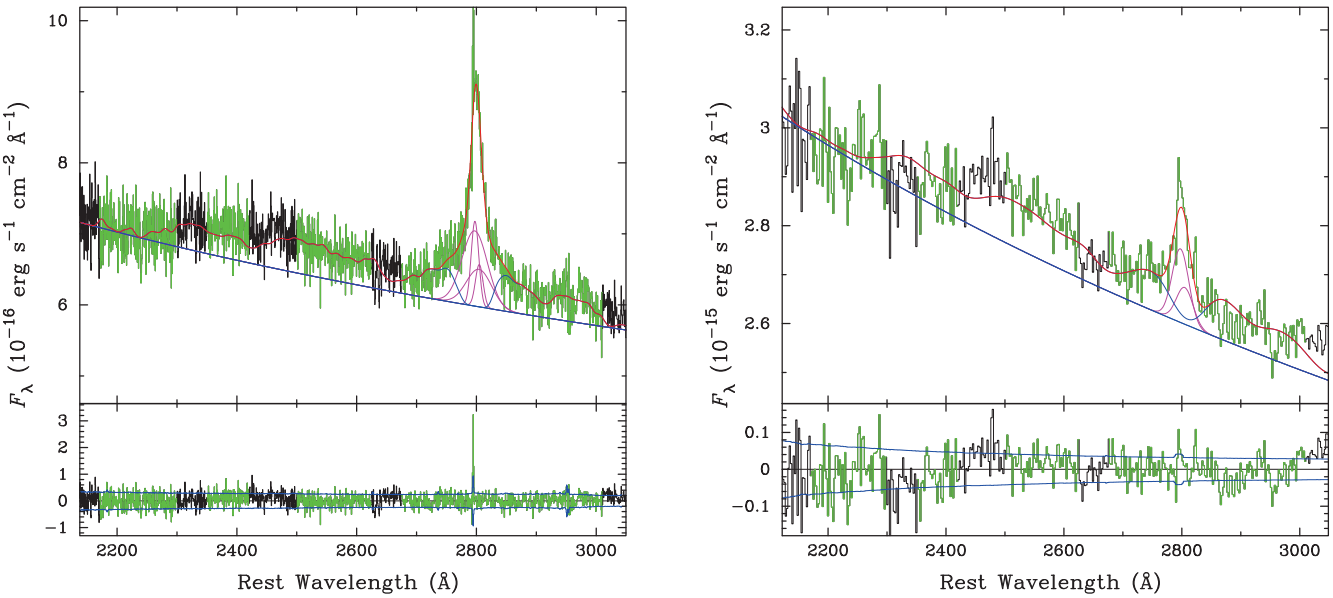

Figure 3. A fit to the spectra of B2 1308+326. Left panel: SDSS spectrum. Right panel: CAHA spectrum.

Table 1
Results of Spectral Fitting

Spectra	Date of Observation	F_{3000}	PL index	$F_{\rm Mg\ II}$	$\rm EW_{Mg\ II}$ (Å)	FWHM (km s^{-1})	$F_{\rm FeII}$
SDSS	2006 March 25	5.71 ± 0.08	−0.67 ± 0.02	112.93 ± 8.28	19.78 ± 1.48	2499.43 ± 120.20	1.34 ± 0.11
CAHA	2024 June 18	25.01 ± 0.22	−0.54 ± 0.01	79.99 ± 6.31	3.20 ± 0.25	3422.16 ± 250.97	2.72 ± 0.38

Note. The continuum fluxes are in the units of 10^{-16} erg cm^{-2} s^{-1} Å^{-1}, the Mg II line fluxes are in the units of 10^{-16} erg cm^{-2} s^{-1}, and Fe II line fluxes are in units of 10^{-14} erg cm^{-2} s^{-1}.

R. J. McLure & M. J. Jarvis 2002; M. S. Shaw et al. 2012)

$$\log\left(\frac{M_{\rm BH}}{M_\odot}\right) = a + b\log\left(\frac{\lambda L_\lambda}{10^{44}\ {\rm erg\ s^{-1}}}\right) + 2\log\left(\frac{\rm FWHM_{MgII}}{\rm km\ s^{-1}}\right), \quad (2)$$

where the coefficients a and b are calibrated using the reverberation mapping data.

Since in blazars (or jetted AGN, in general), the UV/optical emission can be contaminated by the nonthermal jet emission (e.g., X. B. Wu et al. 2004; Y. Liu et al. 2006), in Equation (2) we used $L_{\rm MgII}$ instead of λL_λ and adopted the corresponding coefficients ($a = 1.70$, $b = 0.63$) from M. S. Shaw et al. (2012) to obtain $\rm M_{BH}$. From $\rm M_{BH}$, we got the Eddington luminosity as $L_{\rm Edd} = 1.26 \times 10^{38}\ \rm M_{BH}/M_\odot\ erg\ s^{-1}$.

The luminosity of the AD, $L_{\rm AD}$, can be obtained from $L_{\rm MgII}$, using the following scaling relationship (e.g., M. Zamaninasab et al. 2014):

$$\log L_{\rm AD} = (16.76 \pm 0.26) + (0.68 \pm 0.01)\log L_{\rm MgII}. \quad (3)$$

We then computed the ratio $\lambda = L_{\rm AD}/L_{\rm Edd}$. The measured values of $\rm M_{BH}$, $L_{\rm AD}$, and λ for the two spectra are given in Table 2. Considering the significant uncertainties in the measurement of FWHM of the Mg II line, the values of $\rm M_{BH}$ are consistent for the two spectra. The values of $L_{\rm AD}$ are also marginally different for the two spectra. Both λ values are larger than 10^{-2}, the threshold limit for a blazar to be categorized as an FSRQ.

Table 2
The Measured Values of the Luminosity of Mg II Line ($L_{\rm MgII}$), Black Hole Mass ($M_{\rm BH}$), AD Luminosity ($L_{\rm AD}$), and the Ratio $L_{\rm AD}/L_{\rm Edd}$ for the Two Spectra

Spectra	$\log L_{\rm MgII}$ (erg s^{-1})	$\log M_{\rm BH}$ ($M_\odot$)	$\log L_{\rm AD}$ (erg s^{-1})	$\lambda = L_{\rm AD}/L_{\rm Edd}$
SDSS	43.77 ± 0.07	8.35 ± 0.11	46.53 ± 0.26	1.18 ± 0.76
CAHA	43.62 ± 0.08	8.53 ± 0.15	46.42 ± 0.26	0.62 ± 0.43

4. Discussion

A transition from one class to another has been observed in several blazars by observing changes in either the EW of BELs or in the synchrotron peak frequency. Blazar B2 1308+326 underwent a transition from FSRQ to BL Lac category, which we identified by measuring an order of two shifts in its synchrotron peak frequency in our previous work (Paper I). A similar change in its synchrotron peak frequency was also noticed by D. Watson et al. (2000). In this study, we investigated the transitional behavior of B2 1308+326 by analyzing two of its spectra, obtained with SDSS on MJD 53819 and with CAHA on MJD 60479. The rest-frame UV spectra of B2 1308+326 are characterized by the underlying PL continuum, broad Mg II line, and Fe II emission. We found that the value of continuum flux at 3000 Å is increased from $(5.71 \pm 0.08) \times 10^{-16}$ on MJD 53819 to $(25.01 \pm 0.22) \times 10^{-16}$ erg cm^{-2} s^{-1} Å^{-1} on MJD 60479, accompanied by a change in the PL index from −0.67 to −0.54. However, the Mg II line flux decreased from $(112.93 \pm 8.28) \times 10^{-16}$ to $(79.99 \pm 6.31) \times 10^{-16}$ erg cm^{-2} s^{-1} by a factor of 1.4 ± 0.2,

considering uncertainty (~10%) in the photometric calibration. Due to this enhancement in the continuum flux by a factor of ~4.4 and a decrease in Mg II line flux by a factor of ~1.4, the EW_{MgII} is decreased by a factor of ~6 from (19.78 ± 1.48) to (3.20 ± 0.25) Å. Such a change in the EW_{MgII} may indicate that the source shifted from FSRQ (EW ⩾ 5 Å) to BL Lac class (EW < 5 Å). Different values of EW_{MgII} were reported, separately, for B2 1308+326 in the literature. J. S. Miller et al. (1978) observed $EW_{MgII} < 5$ Å, while no emission lines were detected by B. J. Wills & D. Wills (1979). The larger values of EW_{MgII} ~ 18.6 and ~15 Å were reported by M. Stickel et al. (1993) and D. Watson et al. (2000), respectively, during the low-luminosity states of the source. In this work, we also noticed that when the source was in a low state (MJD 53819), the $EW_{MgII} \geqslant 5$ Å, which was reduced to $EW_{MgII} < 5$ Å when the source continuum increased. Thus, changes in the emission-line properties of B2 1308+326 are predominantly due to the variations in its nonthermal jet continuum, which consequently lead to an apparent change in its class.

To further investigate the intrinsic nature of B2 1308+326, we computed the ratio $\lambda = L_{AD}/L_{Edd}$. A value of $\lambda \geqslant 10^{-2}$ indicates that the AD is radiatively efficient to produce strong emission lines in the spectra and thereby represents an FSRQ source (G. Ghisellini et al. 2011). However, $\lambda < 10^{-2}$ indicates radiatively inefficient accretion, meaning that there are weak or no emission lines, which points to a BL Lac source. We observed that $\lambda > 10^{-2}$ for both the spectra of B2 1308+326 considered in this work. Thus, B2 1308+326 is intrinsically an FSRQ source that shows an apparent change from one class to another due to the fluctuations in its nonthermal jet continuum, thereby pretending to be a CLB.

We used the luminosity and FWHM of the Mg II line to calculate the M_{BH} of B2 1308+326 under the assumption of a virialized BLR. For the SDSS and CAHA spectra, the logarithmic values of M_{BH} are 8.35 ± 0.11 and 8.53 ± 0.15 $M_{\odot}$, respectively, which are comparable within the uncertainties. A slight increase in the velocity (FWHM) of the Mg II line could be due to the decrease in the Mg II line flux, which consequently decreases the radius of the Mg II line–forming region ($R \propto L^{1/2}$; M. Zajaček et al. 2020).

Additionally, we observed that, in contrast to the decline in the Mg II line flux, there is a hint of a slight increase in the Fe II flux with increasing continuum flux level, going from (1.34 ± 0.11) × 10^{-14} to (2.72 ± 0.38) × 10^{-14} erg cm^{-2} s^{-1} by a factor of 2 ± 0.3. As the Fe II flux measurements are highly sensitive to the assumed continuum level, particularly in spectra with moderate S/N and spectral resolution, higher-quality spectra could help to confirm this opposing behavior in Mg II and Fe II flux levels. A similar trend was also observed in the CLB B2 1420+32 by MAGIC Collaboration et al. (2021) and H. D. Mishra et al. (2021). This is an unusual behavior that might point to two distinct emitting regions for the Mg II and Fe II lines. It also suggests that the Fe II emitting gas may align close to the observer's line of sight and thereby interact with the jet emission. Another possible explanation for this unusual trend is that the dusty clouds may undergo sublimation with rising continuum flux, releasing a substantial amount of iron (Fe) into the surrounding environment (H. D. Mishra et al. 2021).

5. Summary

In Paper I, we noticed that the synchrotron peak frequency of B2 1308+326 has shifted from $10^{12.9}$ to $10^{14.8}$ Hz during a flare, providing a hint that it could be a CLB. In this work, we observed a new spectrum of B2 1308+326 with the CAHA telescope and compared it with an archival SDSS spectrum to investigate its changing-look behavior. The key findings of this work are as follows.

1. During the two epochs, the continuum flux (which is possibly a combination of thermal AD flux and nonthermal jet continuum) has increased by a factor of ~4.4, while the Mg II line flux has decreased by a factor of ~1.4.
2. The EW of the Mg II line decreased from ~20 to ~3 Å, indicating an apparent change from FSRQ to BL Lac class.
3. However, the value of the ratio $\lambda = L_{AD}/L_{Edd}$ remains $>10^{-2}$ for the two spectra, representing an efficient accretion in the source. Thus, the blazar B2 1308+326 is intrinsically an FSRQ, and the apparent change from FSRQ to BL Lac class is due to the increased nonthermal jet continuum that diluted the emission lines.
4. Considering measurement uncertainties, the black hole mass of B2 1308+326 is consistent for the two spectra, with an average value of $\log M_{BH} = 8.44\, M_{\odot}$.
5. The Fe II flux has marginally increased by a factor of ~2 with an increase in the continuum flux.

We propose that the blazar B2 1308+326 should not be regarded as a true CLB but rather as an FSRQ that masquerades as a BL Lac source during high-flux states.

Acknowledgments

We thank the referee for the useful comments and suggestions, which have helped improve the clarity and quality of our manuscript. This work is based on observations collected at the Centro Astronómico Hispano en Andalucìa (CAHA) at Calar Alto, operated jointly by the Andalusian Universities and the Instituto de Astrofisica de Andalucìa (CSIC). A.P. acknowledges funding from the Chinese Academy of Sciences President's International Fellowship Initiative (PIFI), grant No. 2024PVC0088. This research is supported by the National Key R&D Program of China (2021YFA1600404 and 2023YFA1607904) and by the National Science Foundation of China (NSFC; 11833008, 11991050, 12122305, and 12333003).

Facility: Sloan

Software: IRAF (D. Tody 1986)

Appendix
Line Flux Measurement Using Simple Integration

We measured the Mg II line flux using simple integration (see Figure 4). First, we established the continuum level by selecting two wavelength windows (shown as blue dashed lines) at 2700–2735 and 2865–2900 Å in the rest frame around the Mg II line. Then, we summed the flux above this continuum within the emission-line window of 2765–2835 Å (indicated by red solid lines). The estimated integrated flux is (7.3 ± 0.4) × 10^{-15} erg cm^{-2} s^{-1}.

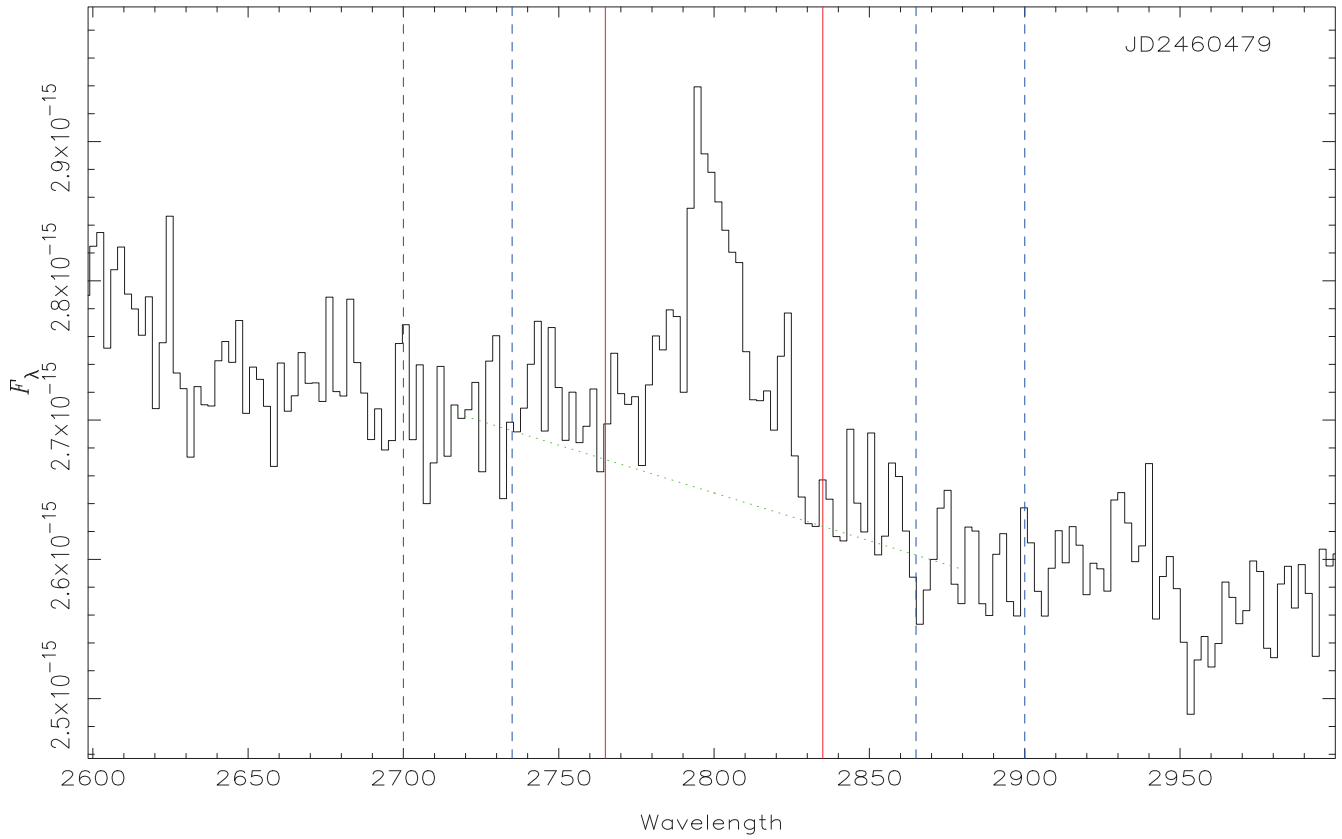

Figure 4. Rest-frame spectra of B2 1308+326. Vertical blue dashed lines show the continuum windows, while the red solid lines indicate the Mg II line window.

ORCID iDs

Ashwani Pandey https://orcid.org/0000-0003-3820-0887
Jian-Min Wang https://orcid.org/0000-0001-9449-9268
Bożena Czerny https://orcid.org/0000-0001-5848-4333
Yong-Jie Chen https://orcid.org/0000-0003-4280-7673
Yu-Yang Songsheng https://orcid.org/0000-0003-4042-7191
Hao Zhang https://orcid.org/0000-0002-5595-0447
Jesús Aceituno https://orcid.org/0000-0003-0487-1105

References

Abdo, A. A., Ackermann, M., Agudo, I., et al. 2010, ApJ, 716, 30
Antonucci, R. 1993, ARA&A, 31, 473
Baldwin, J. A., Ferland, G. J., Korista, K. T., Hamann, F., & LaCluyzé, A. 2004, ApJ, 615, 610
Baldwin, J. A., Ferland, G. J., Korista, K. T., et al. 1996, ApJ, 461, 664
Ghisellini, G., Tavecchio, F., Foschini, L., Bonnoli, G., & Tagliaferri, G. 2013, MNRAS, 432, L66
Ghisellini, G., Tavecchio, F., Foschini, L., & Ghirlanda, G. 2011, MNRAS, 414, 2674
Hewett, P. C., & Wild, V. 2010, MNRAS, 405, 2302
Hu, C., Wang, J.-M., Ho, L. C., et al. 2008, ApJ, 687, 78
Hu, C., Wang, J.-M., Ho, L. C., et al. 2012, ApJ, 760, 126
Hu, C., Li, S.-S., Guo, W.-J., et al. 2020, ApJ, 905, 75
Hu, C., Li, S.-S., Yang, S., et al. 2021, ApJS, 253, 20
Liu, Y., Jiang, D. R., & Gu, M. F. 2006, ApJ, 637, 669
MAGIC Collaboration, Acciari, V. A., Ansoldi, S., et al. 2021, A&A, 647, A163
McLure, R. J., & Jarvis, M. J. 2002, MNRAS, 337, 109
Miller, J. S., French, H. B., & Hawley, S. A. 1978, in BL Lac Objects, ed. A. M. Wolfe (Pittsburgh, PA: Univ. Pittsburgh), 176
Mishra, H. D., Dai, X., Chen, P., et al. 2021, ApJ, 913, 146
Padovani, P. 2017, NatAs, 1, 0194
Paiano, S., Falomo, R., Treves, A., Scarpa, R., & Sbarufatti, B. 2024, ApJ, 968, 81
Pandey, A., Kushwaha, P., Wiita, P. J., et al. 2024, A&A, 681, A116
Ricci, C., & Trakhtenbrot, B. 2023, NatAs, 7, 1282
Ruan, J. J., Anderson, S. F., Plotkin, R. M., et al. 2014, ApJ, 797, 19
Schlafly, E. F., & Finkbeiner, D. P. 2011, ApJ, 737, 103
Shaw, M. S., Romani, R. W., Cotter, G., et al. 2012, ApJ, 748, 49
Shen, Y., Richards, G. T., Strauss, M. A., et al. 2011, ApJS, 194, 45
Stickel, M., Fried, J. W., & Kuehr, H. 1993, A&AS, 98, 393
Stocke, J. T., Morris, S. L., Gioia, I. M., et al. 1991, ApJS, 76, 813
Tody, D. 1986, Proc. SPIE, 627, 733
Urry, C. M., & Padovani, P. 1995, PASP, 107, 803
Vestergaard, M., & Wilkes, B. J. 2001, ApJS, 134, 1
Watson, D., Smith, N., Hanlon, L., et al. 2000, A&A, 364, 43
Wills, B. J., & Wills, D. 1979, ApJS, 41, 689
Wu, X. B., Wang, R., Kong, M. Z., Liu, F. K., & Han, J. L. 2004, A&A, 424, 793
Zajaček, M., Czerny, B., Martinez-Aldama, M. L., et al. 2020, ApJ, 896, 146
Zamaninasab, M., Clausen-Brown, E., Savolainen, T., & Tchekhovskoy, A. 2014, Natur, 510, 126